Table I. Summary of Representative Vibrational Frequencies (cm^{-1}) Observed for $Os^{III}(NH_3)_5py$, $Os^{II}(NH_3)_5py$, and Pyridine at Silver Electrodes and in Bulk Media[a]

$Os(NH_3)_5py$						
IR[b]	IR[b]	Raman[c]	SERS[d]		pyridine	
Os(III)	Os(II)	Os(III)	−150 mV	−750 mV	SERS[g]	assignment[h]
			291 w	267 m		Os–py stretch
		501 w	494 w	468 m		Os–NH_3 stretch
		654 w	653 m	648 s	625 w,[e] 623[f]	in-plane ring deformation
1022 m	990 m	1020 s	1020 vs	992 s	1007 vs,[e] 1007[f]	sym ring breathing
1055 w	1055 w		1050 m	1053 s	1035 s,[e] 1035[f]	trigonal ring breathing

[a] vs = very strong, s = strong, m = medium, w = weak. [b] Infrared data obtained by using $Os(NH_3)_5py{\cdot}I_3$ and $Os(NH_3)_5py{\cdot}I_2$ in CsI pellets. [c] Normal Raman data obtained by using $Os(NH_3)_5py{\cdot}Cl_3$ in KBr pellets. [d] Surface-enhanced Raman vibrational modes for electrochemically roughened silver electrode in 0.1 M NaBr + 0.1 M HCl + 0.1 mM $Os(NH_3)_5py^{3+}$ at indicated potentials vs. SCE. [e] From this work, for 10 mM pyridine in 0.1 M NaBr. [f] From ref 10, for 50 mM pyridine in 0.1 M KCl. [g] Frequencies were potential independent (±2 cm^{-1}) from −150 to −750 mV. [h] See text for details.

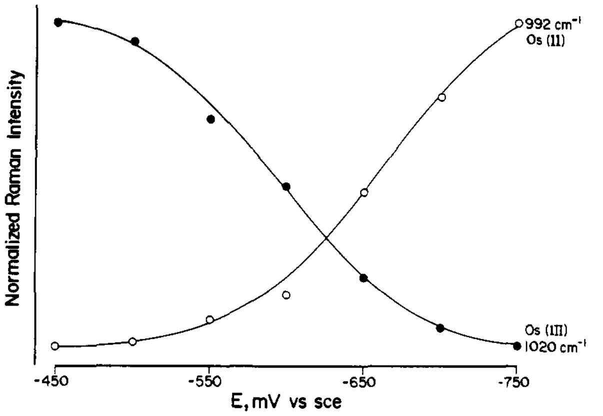

Figure 2. Normalized intensity of the symmetric ring breathing mode as a function of electrode potential. Osmium oxidation states are indicated. Data are as in Figure 1.

Indeed, an almost identical frequency shift in this mode is seen for the infrared spectra of the bulk Os(III) and Os(II) complexes (Table I).

Using rapid-scan cyclic voltammetry (50–100 V s^{-1}) and very dilute $Os(NH_3)_5py^{3+}$ concentrations (~50 μM),[13] the formal potential of the adsorbed Os(III)/(II) couple, E_f^a, was found to be −670 mV in 0.1 M HCl at roughened silver, (cf. the formal potential for the bulk couple, E_f^b = −655 mV). Moderate adsorption (~(3–4) × 10^{-11} mol cm^{-2}) was indicated by the charge underneath the almost symmetric cyclic voltammograms. Formal potentials, E_f^a, were also determined from the SERS intensity–potential data. Figure 2 shows the potential dependence of the normalized integrated intensities of the 1020- and 992-cm^{-1} SERS ring breathing modes in the vicinity of E_f^a. Assuming the intensities are proportional to the corresponding surface concentrations, a Nernstian treatment[3] gave values of E_f^a (−630 ± 10 mV), similar to those determined electrochemically.

The appearance of SERS signals for the present system is in itself noteworthy since coordinated pyridine is unable to bind to the surface via the nitrogen lone pair. Such surface coordination is often regarded as a preprequisite for the appearance of SERS for adsorbed pyridine.[4a] Adsorption of the coordinated pyridine is likely to occur edgewise via a C=C bond;[14] the alternative flat orientation will be sterically hindered by the presence of the coordinated pentaammineosmium. Direct metal–pyridine bonding is also consistent with the excellent mediating properties of coordinated pyridine for pentaamminecobalt(III) reduction at metal surfaces.[15] Nevertheless, the adsorbate–electrode interactions are presumably weak, as evidenced by the similarity of E_f^a and E_f^b, and the vibrational frequencies of $Os(NH_3)_5py$ III/II at the surface and in bulk media. SERS of osmium and ruthenium complexes containing coordinated pyrazine and 4,4′-bipyridine ligands that are able to bind to the surface via the exposed nitrogen, thereby yielding stronger adsorbate–surface interactions, will be described elsewhere.[3]

The present results illustrate the potential of SERS for monitoring heterogeneous electron-transfer processes and suggest that adsorbates bound to SERS-active sites are energetically similar to those observed by conventional electrochemistry.

Acknowledgment. We thank George Leroi for the use of the Raman spectrometer. Some preliminary experiments were performed by Ken Guyer, and the electrochemical measurements by Joe Hupp. The research program of M.J.W. is supported in part by the Office of Naval Research and the Air Force Office of Scientific Research, and of H.T. by the NSF (Grant CHE 79-08633) and NIH (Grant GM 13638-17). P.A.L. gratefully acknowledges a CSIRO Postdoctoral Fellowship, and M.J.W. a Sloan Foundation Fellowship.

Registry No. $[Os(NH_3)_5py]Cl_3$, 70252-36-7; $Os^{II}(NH_3)_5py$, 70252-47-0; Ag, 7440-22-4.

---

[12] Taube, H. *Pure Appl. Chem.* **1979**, *51*, 901.

[13] Guyer, K. L.; Barr, S. W.; Weaver, M. J. "Proceedings of the Symposium on Electrocatalysis"; O'Grady, W. E., Ross, P. N., Jr., Hill, F. G., Eds.; The Electrochemical Society: Pennington, NJ, 1982; p 377.

[14] Conway, B. E.; Mathieson, J. G.; Dhar, H. P. *J. Phys. Chem.* **1974**, *78*, 1226. Soriaga, M. P.; Hubbard, A. T. *J. Am. Chem. Soc.* **1982**, *104*, 2735.

[15] Srinivasan, V.; Barr, S. W.; Weaver, M. J. *Inorg. Chem.* **1982**, *21*, 3154.

Circularly Polarized Fluorescence of Aromatic Poly(α-amino acids)

Masahiko Sisido,*† Syun Egusa, Akira Okamoto, and Yukio Imanishi

Research Center for Medical Polymers and Biomaterials
and Department of Polymer Chemistry, Kyoto University
Kyoto 606, Japan

Received November 24, 1982

This communication describes studies of circularly polarized fluorescence (CPF) of aromatic poly(α-amino acids) having 1- and 2-naphthyl and 9-anthryl groups on their side chains. The nature of monomer, excimer, and exciton fluorescence state is discussed on the basis of the dissymmetry of fluorescence.

Aromatic poly(α-amino acids) such as poly(L-1- and 2-naphthylalanines)[1,2] (poly(1- and 2-NapAla)) and poly(anthrylmethyl L-aspartate)[3] (poly[Asp(OCH_2-9-Ant)]) have been prepared with an expectation that they may work as a molecular conductor that can transport electrons across biological mem-

---

† To whom correspondence should be addressed at the Research Center for Medical Polymers and Biomaterials.

[1] Sisdo, M.; Egusa, S.; Imanishi, Y. *J. Am. Chem. Soc.* **1983**, *105*, 1041.

[2] Sisido, M.; Egusa, S.; Imanishi, Y. *J. Am. Chem. Soc.*, in press. Poly(2-NapAla) showed an exciton splitting in the CD spectrum at the ^1B_b band ($[\theta]_{234}$ = 6.0 × 10^5, $[\theta]_{219}$ = −2.3 × 10^5 deg cm^2 $dmol^{-1}$) in trimethyl phosphate.

[3] Poly[Asp(OCH_2-9-Ant)] was prepared from Asp(OCH_2-9-Ant) NCA. The polymer showed an exciton splitting at the ^1B_b band ($[\theta]_{265}$ = −1.9 × 10^5, $[\theta]_{235}$ = 2.8 × 10^5, deg cm^2 $dmol^{-1}$) in trimethyl phosphate.

0002-7863/83/1505-3351$01.50/0

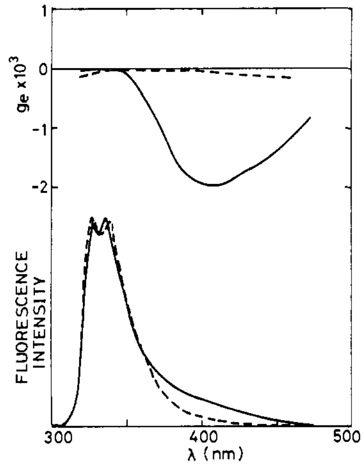

Figure 1. Fluorescence (bottom) and CPF (top) spectra of poly(1-NapAla) (---) and poly(2-NapAla) (—) in N_2-bubbled dimethylformamide ([Nap] = 3.0 × 10^{-4} M).

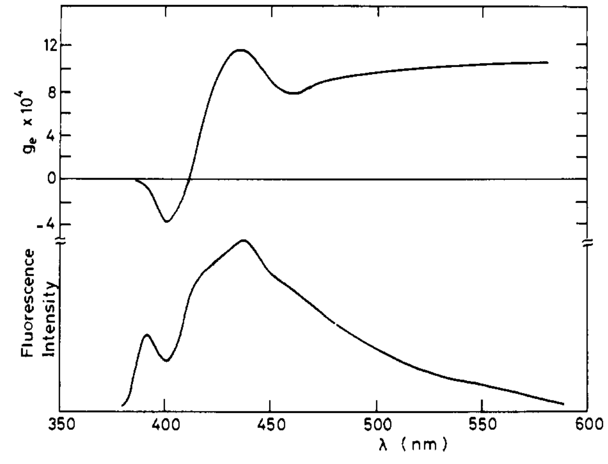

Figure 2. Fluorescence (bottom) and CPF (top) spectra of poly[Asp(OCH_2-9-Ant)] in N_2-bubbled trimethyl phosphate ([Ant] = 2.7 × 10^{-4} M).

brane.[1] UV, CD, and fluorescence spectroscopy revealed that the aromatic chromophores in these polymers are helically arranged and form exciton states at the ^1B_b excited states as a result of long-range dipole–dipole interactions, but the excimer formation is suppressed to a minimum extent, probably because the helix-bound chromophores cannot approach each other within ca. 3.5 Å.[1,2] The following two points, however, remain to be clarified: (1) whether the polymeric excited state of the lowest energy is delocalized over chromophores as an exciton state[4] or virtually localized on a monomeric unit; (2) whether excimers can be formed between a pair of the helix-bound chromophores. To answer these questions, CPF spectra were measured, since they reflect the dissymmetry of the excited state.[5,6] The exciton fluorescence or excimer fluorescence of the helix-bound chromophores may show large dissymmetry, whereas the localized excited state may show little or no CPF signal, even if the chromophores are bound to asymmetric polymer chains.[5]

Three kinds of poly(α-amino acids) were prepared by the polymerization of corresponding α-amino acid N-carboxyanhydrides (NCA's) with preformed poly(γ-benzyl DL-glutamate) as a soluble initiator fragment.[1-3] The CPF instrument was designed according to Steinberg and Gafni[7] and assembled by Japan Spectroscopic Co. (Hachioji, Tokyo).[8]

Figure 1 shows fluorescence (bottom) and CPF (top) spectra of poly(1- and 2-NapAla) in N_2-bubbled dimethylformamide. The ordinate of the CPF spectrum is represented by Kuhn's dissymmetry factor, $g_e = 2(I_L - I_R)/(I_L + I_R)$. No CPF signal was detected at the monomer fluorescence region of the two poly(NapAla's). This indicates that the polymeric fluorescent state is virtually localized on a monomeric naphthyl group. The result is reasonable, since the fluorescence transition of the naphthyl group (^1L_b) is forbidden and no dipole–dipole interaction is possible between chromophores. In the absorption circular dichroism of the two polymers, an intense exciton splitting has been observed in the ^1B_b band, which has a large transition dipole moment.[1,2] It is concluded that although the ^1B_b excited state forms an exciton state, the lowest energy ^1L_b stte is localized on a monomeric unit.

Alternatively, the absence of the dissymmetry in monomer fluorescence could be interpreted by a frequent energy migration among the helix-bound chromophores and an efficient entrapping of the energy into an isolated chromophore at the chain end. The latter fluoresces without dissymmetry. The decay curve of the monomer fluorescence of poly(1-NapAla) consisted of two components with τ = 14 (fraction = 0.32) and 50 ns (0.68). The former may be assigned to the fluorescence from the helical part and the latter from the isolated chromophore. Therefore, if the former had a significant g_e value, one should have observed a definite CPF signal, which was not the case.

In the excimer region of CPF spectrum, poly(1-NapAla) showed no dissymmetry, whereas the 2-naphthyl polymer exhibited a large CPF signal. The former result indicates that the excimer formation in poly(1-NapAla) is absolutely prohibited or only possible at the chain ends where chromophores are randomly oriented. The large excimer dissymmetry in poly(2-NapAla) suggests that the geometry of the helix-bound chromophores can fluctuate to form skewed excimer sites in the polymer.

Since the fluorescent state of anthracene (^1L_a) has a large transition dipole moment, a fluorescence emission from an exciton state is expected for poly[Asp(OCH_2-9-Ant)]. A small but definite CPF signal is observed at the monomer fluorescence region in Figure 2. Since the corresponding monomeric compound, N-(benzyloxycarbonyl)-β-(9-anthrylmethyl)-α-benzyl L-aspartate, showed no CPF signal, the above observation indicates that the "monomer" fluorescence state is actually an exciton state, although the extent of the delocalization may not be large.

At the excimer fluorescence region, two fluorescence transitions having different g_e values are detected. the shorter wavelength region may be assigned to a second excimer that has been considered to have a small overlapping area between the two chromophores.[9,10] In the present case two anthryl groups might take an asymmetrically skewed configuration overlapping partially with each other. The excimer fluorescence at longer wavelengths having a constant g_e value may be assigned to a sandwichlike excimer. However, since its fluorescence shows a significant dissymmetry, its configuration may also be asymmetrically twisted from the symmetric sandwich configuration.

Acknowledgment. We are grateful to Professor Y. Shindo of Fukui University for giving information on the CPF instrument.

---

(4) Davydov, A. S. "Theory of Molecular Excitons"; Plenum Press: New York, 1971.

(5) Richardson, F. S.; Riehl, J. P. *Chem. Rev.* **1977**, *77*, 773.

(6) Steinberg, I. Z. *Ann. Rev. Biophys. Bioeng.* **1978**, *7*, 113.

(7) Steinberg, I. Z.; Gafni, A. *Rev. Sci. Instrum.* **1972**, *43*, 409.

(8) The CPF instrument consists of a 450-W xenon lamp, grating monochromator for exciting light, quartz depolarizer, photoelastic modulator operating at 50 kHz, analyzer, grating monochromator for fluorescence, photomultiplier, preamplifier, lock-in amplifier, and XY recorder. The negative high voltage for the photomultiplier was controlled as to obtain a constant dc output. Therefore, the 50-kHz ac output is directly proportional to the Kuhn's dissymmetric factor, which was amplified by the lock-in amplifier and recorded on an XY recorder as a function of the fluorescence wavelength. It was necessary to insert appropriate solution filters in the excitation light beam to eliminate a trace of stray light.

(9) (a) Johnson, G. E. *J. Chem. Phys.* **1975**, *62*, 4697. (b) Itaya, A.; Okamoto, K.; Kusabayashi, S. *Bull. Chem. Soc. Jpn.* **1978**, *51*, 79. (c) Hoyle, C. E.; Nemzek, T. L.; Mar, A.; Guillet, J. E. *Macromolecules* **1978**, *11*, 429. (d) Johnson, G. E.; Keyanpour-Rad, M.; Ledwith, A. *Ibid.* **1980**, *13*, 222. (e) Roberts, A. J.; Phillips, D.; Abdul-Rasoul, A. M.; Ledwith, A. *J. Chem. Soc., Faraday Trans. 1* **1981**, *77*, 2725. (f) Gupta, A.; Liang, R.; Moacanin, J.; Kliger, D.; Goldbeck, R.; Horwitz, J.; Miskowski, V. M. *Eur. Polym. J.* **1981**, *17*, 485.

(10) (a) Itoh, M.; Fuke, K.; Kobayashi, S. *J. Chem. Phys.* **1980**, *72*, 1417. (b) Itagaki, H.; Obukata, N.; Okamoto, A.; Horie, K.; Mita, I. *J. Am. Chem. Soc.* **1982**, *104*, 4469